

HOMOGENIZATION OF THREE-DIMENSIONAL MICRO-HETEROGENEOUS MATERIALS USING NONUNIFORM TRANSFORMATION FIELDS

Felix Fritzen and Thomas Böhlke

Chair of Continuum Mechanics, Institut of Engineering Mechanics,
University of Karlsruhe (TH), Post box 6980, 76128 Karlsruhe, Germany,
e-mail: fritzen@itm.uni-karlsruhe.de

Keywords: Homogenization, Mesh generation, Metal Matrix Composites (MMC), Nonuniform Transformation Field Analysis (NTFA)

Abstract. *The inelastic material properties of Metal Matrix Composites (MMC) with particulate reinforcement are investigated. In order to be able to investigate a variety of unit cells a method for the generation and spatial discretization of random model microstructures is presented. The Nonuniform Transformation Field Analysis (NTFA) is employed to investigate the properties of the microheterogeneous material with physical non-linearity. The coefficients of the NTFA are determined from full-field simulations using the Finite Element Method (FEM) on the microscopic scale with consideration of the exact geometry. The homogenized material model is implemented into ABAQUS STANDARD. Numerical examples highlight the efficiency of the method.*

1 INTRODUCTION

Many materials consist of multiple constituents on the microscopic scale. This micro-heterogeneity often influences the macroscopic properties. For example, modern composite materials consisting of a metallic matrix and ceramic reinforcement have shown favorable mechanical and thermo-mechanical properties that are governed by the individual physical properties and the geometry of the reinforcement.

A variety of homogenization methods has been proposed in the past century (see e.g. Nemat-Nasser and Hori [1]) for the linear mechanical and thermal properties of microheterogeneous materials. The latter can be considered to be (mostly) well understood for many materials. Some established analytical and semi-analytical methods for the homogenization of linear properties are the upper Voigt bound and the lower Reuss bound, the Hashin-Shtrikman bounds [2], the Mori Tanaka estimate [3] and self-consistent estimates [4]. Numerical computations have shown that these methods can determine the linear properties of many microheterogeneous materials to a sufficient extent (e.g. Fritzen et al. [5]) if the contrast in the physical properties is small or moderate.

In practice many materials show non-linearities such as plasticity, damage and fracture. When non-linear material properties are investigated many of the assumptions entering the aforementioned methods are no longer satisfied. Particularly, the stress and strain fields become nonlinear functions of the macroscopic loading with a (mostly) unknown structure of the macroscopic constitutive equations. The evolution of inelasticity cannot be determined (semi-)analytically due to severe path-dependency except in rare cases. Numerical methods based on the Finite Element Method (FEM), the Fast Fourier Transform (FFT), the Boundary Element Method (BEM) and others have employed to determine the effective behaviour of non-linear heterogeneous materials. One of the numerical multiscale methods is the multi-level Finite Element Method (FE^p) in which each integration point in a finite element analysis is equipped with a sub-grid containing the full information of the microscopic constituent. The method has seen massive attention for two-dimensional problems (e.g. Miehe [6]) and the technique has been extended to generalized continua by Feyel [7]. The large degree of freedom with respect to the modelling of materials and structures when using a multi-level FE approach in return leads to an excessive number of degrees of freedom even for two-dimensional problems. Application to three-dimensional problems is still limited, despite the ever increasing amount of available memory and CPU power. It has to be mentioned that, usually, FE^p requires massive parallelization which precludes application of the method for many engineers in industry and research facilities.

In order to condense the number of degrees of freedom Dvorak and Benveniste [8], Dvorak et al. [9] proposed the Transformation Field Analysis (TFA). In the latter the plastic strain field is assumed to be constant in subdomains of the microscopic material. Hence, only few coefficients need to be computed. The method has been applied for the homogenization of non-linear material properties of materials at acceptable numerical cost. However, the method has been shown to overestimate significantly the stiffness of the microstructure [10].

Michel and Suquet [11] extended the TFA to the case of plastic strain fields which are no longer piecewise constant in order to overcome the overly stiff predictions of the effective material response. More precisely, the characteristic deformation patterns of composite structures can be replicated using only few scalar coefficients. The method has been applied to two-dimensional composites with great success [11, 12, 13].

In this paper the non-uniform transformation field analysis (NTFA) is applied to random three-dimensional model microstructures resembling particulate MMCs in the absence of damage, i.e. linear elastic particles and a ductile matrix material are considered. Section 2 is devoted to the generation of the geometry and the spatial discretization of the latter. In Section 3 the constitutive equations of the NTFA are briefly revisited and equations describing the macroscopic material behaviour using the internal variable formalism are derived. The effective stress-strain response of the homogenized material is compared to the one of full-field unit cell computations under proportional and non-proportional loading in Section 4.

2 MODEL MICROSTRUCTURES

The concept of model microstructures created based on random variables allows to examine a variety of different unit cell problems. As an example model microstructures based on Voronoi tessellations have been used for polycrystalline aggregates in the past (e.g. Barbe et al. [14]) to numerically perform statistical investigations. The authors have recently proposed a fast mesh generator based on the Voronoi tessellation which creates not only periodic microstructures but also periodic mesh topologies while the geometry is exactly replicated [5]. In this section a modification of the procedure is described in order to construct three-dimensional model microstructures consisting of a matrix material and polygonal particulate inclusions. These particle shapes are often found in metal matrix composites reinforced with ceramic powders (see e.g. Miserez et al. [15]).

For simplicity a cuboidal unit cell of the type

$$\Omega = [-w/2, w/2] \times [-d/2, d/2] \times [-h/2, h/2] \subset \mathbb{R}^3 \quad (1)$$

is considered. First, a set of N random points $P_i \in \Omega$ is generated and copied 26 times around the unit cell in order to define a periodic Voronoi tessellation [16]. A point $X \in \Omega$ is part of the Voronoi cell defined by the point P_i which has the smallest (Euclidean) distance to X . The cells of a Voronoi tessellation are convex bounded polyhedra which can either be characterized by their corner vertices or in terms of the intersection of a set of m halfspaces, with m being the number of faces of the cell.

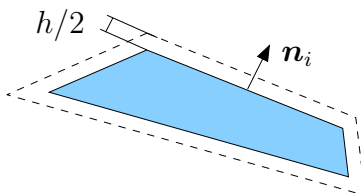


Fig. 1: Shrunked convex polyhedron (here: in 2d)

Each of the halfspaces H_i is characterized by its outward unit normal vector \mathbf{n}_i and the offset δ_i from the origin. Each cell is defined by a set of M tuples $\{\mathbf{n}_i, \delta_i\}_{i=1, \dots, M}$. By

modifying the offset parameters via

$$\delta_i^* = \delta_i - \frac{h}{2} \quad (i = 1, \dots, M), \quad (2)$$

all cell faces are translated in negative unit normal direction, i.e. inwards, forming a separating layer of thickness h between two neighboring cells. The following properties are found for cells constructed by the described methods:

- Cells can vanish during the shrinking process due to their small initial size.
- The remaining cells are convex.
- All cells have a uniform distance to their direct neighbors, i.e. there is no penetration and no percolation.
- The number of faces of the new cell is smaller than or equal to the number of faces on the original cell.
- The volume fraction of the inclusions can be scaled by the parameter h .
- The microstructure is periodic. This allows to endow the unit cell with periodic displacement boundary conditions or anti-periodic traction boundary conditions (e.g. Miehe [6] and others).

With the definition of the faces of the inclusions a periodic three-dimensional mesh can be obtained by the procedure described by Fritzen et al. [5] with minor modifications. Particularly, the filler material has to be added to the mesh and the surface mesh on the faces of the unit cell has to be modelled with care. It is noteworthy that the advantages of the mesh generation algorithm such as fast mesh generation and fully scalable mesh density apply to this new class of model microstructures. Additionally, it is possible to modify the point seed P_i by superimposing a hardcore condition etc., thereby increasing the regularity of the cells.

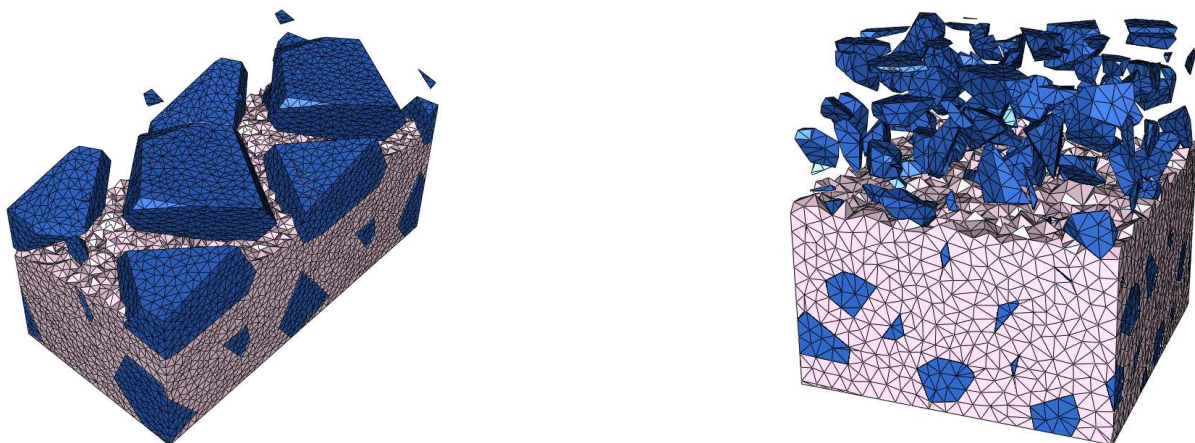


Fig. 2: Example meshes for $N = 5$ (left with periodic continuation), 200 (right)

Example meshes for $N = 5$ and 200 are shown in Fig. 2. Remarkably, the larger the number of inclusions the denser the mesh has to be in order to expect proper results from

a finite element analysis. This may quickly lead to several million degrees of freedom in a mechanical finite element analysis. Hence, such discrete microstructures are not recommended for application with FE^p methods.

3 NONUNIFORM TRANSFORMATION FIELD ANALYSIS

The focus of this paper are two-scale problems in the context of small deformations. The restriction to geometrically linear behaviour is reasonable for many composite materials. On the microscopic scale the stress, strain and the displacement are denoted by $\boldsymbol{\sigma}$, $\boldsymbol{\varepsilon}$ and \mathbf{u} , respectively. Overlined quantities are taken at the macroscopic (structural) level of the domain $\bar{\Omega}$ with boundary $\bar{\Gamma} = \partial\bar{\Omega}$. The macroscopic and the microscopic strain and stress fields are related by the averaging operator $\langle \bullet \rangle = |\Omega|^{-1} \int_{\Omega} \bullet \, dV$:

$$\bar{\boldsymbol{\varepsilon}} = \langle \boldsymbol{\varepsilon} \rangle, \quad \bar{\boldsymbol{\sigma}} = \langle \boldsymbol{\sigma} \rangle. \quad (3)$$

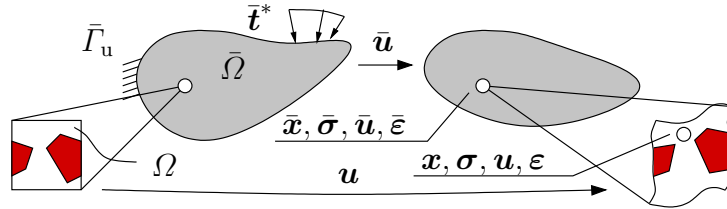


Fig. 3: Macroscopic (structural) problem and associated microscopic problem

Then the homogenization problem persists in solving

$$(\bar{P}) : \begin{cases} \operatorname{div}(\bar{\boldsymbol{\sigma}}) = \mathbf{0} & \text{in } \bar{\Omega}, \\ \bar{\boldsymbol{\sigma}} \bar{\mathbf{n}} = \bar{\mathbf{t}} = \bar{\mathbf{t}}^* & \text{on } \bar{\Gamma}_t \subsetneq \bar{\Gamma}, \\ \bar{\mathbf{u}} = \bar{\mathbf{u}}^* & \text{on } \emptyset \neq \bar{\Gamma}_u \subset \bar{\Gamma}, \end{cases} \quad \text{and } (P) : \begin{cases} \operatorname{div}(\boldsymbol{\sigma}) = \mathbf{0} & \text{in } \Omega, \\ \langle \boldsymbol{\varepsilon} \rangle = \bar{\boldsymbol{\varepsilon}}, \\ \boldsymbol{\sigma} & \text{admissible,} \end{cases} \quad (4)$$

where the admissible domain of $\boldsymbol{\sigma}$ is, e.g., defined by the yield surface of a plastic material.

The major assumption of the NTFA is the existence of a finite dimensional basis spanned by plastic strain fields $\boldsymbol{\mu}^{(i)}(\mathbf{x})$ ($i = 1, \dots, N < \infty$), such that the plastic strain field $\boldsymbol{\varepsilon}^p$ can be approximated by $\boldsymbol{\varepsilon}_{\text{app}}^p$ for some $\delta_p > 0$, such that

$$\boldsymbol{\varepsilon}_{\text{app}}^p(t, \mathbf{x}) = \sum_{i=1}^N \xi_i(t) \boldsymbol{\mu}^{(i)}(\mathbf{x}), \quad \|\boldsymbol{\varepsilon}_{\text{app}}^p(t, \mathbf{x}) - \boldsymbol{\varepsilon}^p(t, \mathbf{x})\| < \delta_p \quad (5)$$

for some suitable norm. The latter usually involves volume averaging. An example is the L^2_{Ω} norm. Obviously (5) cannot be satisfied for arbitrary deformation processes. It can, however, be observed that real materials show characteristic deformation patterns, e.g. plastification in regions between almost rigid inclusions. These characteristic deformations are massively influenced by both, the physical properties of the material (anisotropy, nonlinearity) and the topology of the heterogeneous medium. The latter can for example be described by means of n -point correlation functions [17].

The idea of the NTFA persists in trying to determine (a small but sufficient number of) plastic modes $\boldsymbol{\mu}^{(i)}$ associated with the characteristic deformations of a unit cell in a

numerical testing environment and then to formulate appropriate evolution equations for the coefficients $\xi_i(t)$. The local stress and strain field at position \mathbf{x} and time t can be expressed in terms of $\boldsymbol{\xi}(t)$ and the strain concentration tensor $\mathbb{A}(\mathbf{x})$

$$\boldsymbol{\varepsilon}(\mathbf{x}, t) = \mathbb{A}(\mathbf{x})[\bar{\boldsymbol{\varepsilon}}] + \sum_{j=1}^N \xi_j(t) \boldsymbol{\varepsilon}_*^{(j)}(\mathbf{x}), \quad (6)$$

$$\boldsymbol{\sigma}(\mathbf{x}, t) = \mathbb{C}(\mathbf{x})\mathbb{A}(\mathbf{x})[\bar{\boldsymbol{\varepsilon}}] + \sum_{j=1}^N \xi_j(t) \boldsymbol{\sigma}_*^{(j)}(\mathbf{x}). \quad (7)$$

Following the method introduced by Michel and Suquet [11, 12] the thermodynamic driving forces are:

$$\boldsymbol{\tau}^{(i)} = \langle \mathbb{A}^\top \mathbb{C}[\boldsymbol{\mu}^{(i)}] \rangle \cdot \bar{\boldsymbol{\varepsilon}} + \sum_{j=1}^N \xi_j \langle \boldsymbol{\mu}^{(i)} \cdot \boldsymbol{\sigma}_*^{(j)} \rangle = \langle \mathbb{A}^\top \mathbb{C}[\boldsymbol{\mu}^{(i)}] \rangle \cdot \bar{\boldsymbol{\varepsilon}} + \mathbf{D}\boldsymbol{\xi}, \quad (8)$$

with $\boldsymbol{\sigma}_*^{(j)} = \mathbb{C}[\boldsymbol{\varepsilon}_*^{(j)} - \boldsymbol{\mu}^{(j)}]$ the solution of the eigenstress problem

$$(P_\sigma^j) : \quad \text{div}(\mathbb{C}[\boldsymbol{\varepsilon}_*^{(j)} - \boldsymbol{\mu}^{(j)}]) = \mathbf{0}, \quad \langle \boldsymbol{\varepsilon}_*^{(j)} \rangle = \mathbf{0}. \quad (9)$$

We assert that the modes satisfy the restrictions of [11, 12]:

- The modes are normalized ($\langle \|\boldsymbol{\mu}^{(i)}\|_2 \rangle = 1$).
- The modes are linearly independent and the support of individual modes is restricted to one phase.
- The modes are orthogonal ($\langle \boldsymbol{\mu}^{(i)} \cdot \boldsymbol{\mu}^{(j)} \rangle = 0$ ($i \neq j$)).

A suitable evolution equation for the internal variables ξ_i has been found to be

$$\dot{\xi}_i = \dot{\lambda} \frac{\tau^{(i)}}{\|\boldsymbol{\tau}\|_2} \quad (10)$$

for a material showing plasticity of von Mises type. The variable $\dot{\lambda}$ is a Lagrangian multiplier satisfying the Karush-Kuhn-Tucker complementary conditions

$$\dot{\lambda} \varphi = 0, \quad \dot{\lambda} \geq 0, \quad \text{for } \varphi(\boldsymbol{\tau}, \bar{q}) = \|\boldsymbol{\tau}\|_2 - \sqrt{2/3} \sigma_F(\bar{q}). \quad (11)$$

The variable \bar{q} is an additional internal variable accounting for isotropic hardening effects. The latter is assumed constant over the entire unit cell, i.e. it has a spatially uniform distribution. The evolution equation for the hardening variable is

$$\dot{\bar{q}} = \dot{\lambda} \sqrt{\frac{2}{3}}. \quad (12)$$

As an important outcome of (7), the macroscopic stress $\bar{\boldsymbol{\sigma}}$ is a linear transformation of the macroscopic strain $\bar{\boldsymbol{\varepsilon}}(t)$ and coefficients $\boldsymbol{\xi}(t)$:

$$\begin{aligned} \bar{\boldsymbol{\sigma}}(\bar{\boldsymbol{\varepsilon}}(t), \boldsymbol{\xi}(t)) &= \langle \mathbb{C}(\mathbf{x})\mathbb{A}(\mathbf{x}) \rangle [\bar{\boldsymbol{\varepsilon}}] + \sum_{j=1}^N \xi_j(t) \langle \boldsymbol{\sigma}_*^{(j)} \rangle \\ &= \bar{\mathbb{C}}[\bar{\boldsymbol{\varepsilon}}] + \sum_{j=1}^N \xi_j(t) \langle \boldsymbol{\sigma}_*^{(j)} \rangle. \end{aligned} \quad (13)$$

4 NUMERICAL EXAMPLES

4.1 Comparison on unit cell level

The NTFA is implemented into ABAQUS/STANDARD using an implicit time integration procedure based on the Backward Euler scheme to integrate (11) and (12) on the interval $[t_n, t_{n+1}]$. The microstructure and discretization used in the subsequent analysis are shown in Fig. 4.

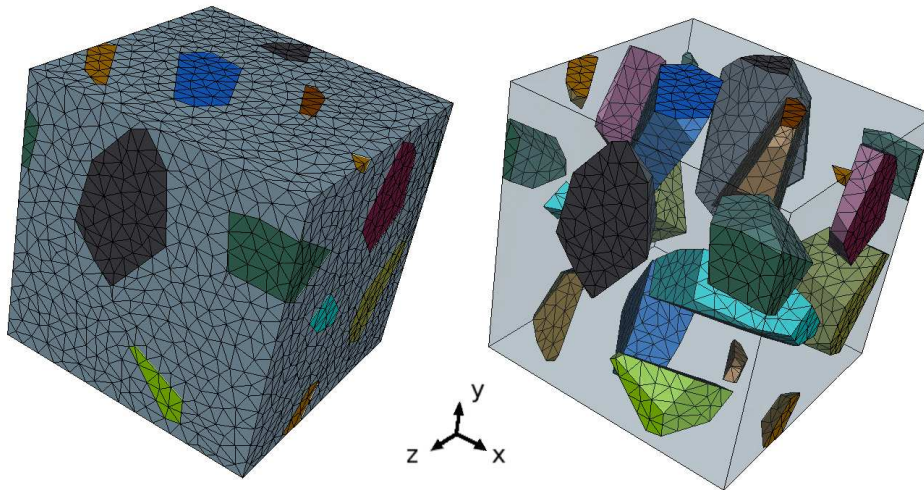


Fig. 4: Discretized model microstructure used in the nonuniform transformation field analysis

As has been shown by Fritzen and Böhlke [18] the behaviour of the unit cell for proportional multi-axial loading can well be approximated by the NTFA when using only a small number of modes. These investigations are continued by examining the behaviour upon nonproportional loading on the unit cell level in a first step. Therefore a strain-path consisting of two different loading directions is prescribed to (i) a full field unit cell computation and (ii) the homogenized material model. The macroscopic stress tensors computed using the two methods are then compared. The strain rate of the process is

$$\dot{\hat{\boldsymbol{\varepsilon}}}_1 = \begin{pmatrix} 1 & 0 & 0 \\ 0 & -1 & 0 \\ 0 & 0 & 0 \end{pmatrix} \frac{\mathbf{e}_i \otimes \mathbf{e}_j}{100\text{s}}, \quad \dot{\hat{\boldsymbol{\varepsilon}}}_2 = \begin{pmatrix} 0 & 0 & 2 \\ 0 & 0.5 & 0 \\ 2 & 0 & -0.5 \end{pmatrix} \frac{\mathbf{e}_i \otimes \mathbf{e}_j}{100\text{s}}. \quad (14)$$

Each of the two rates is held constant for 1 s. A total of only five different modes has been identified for considered model microstructure containing 10 linear elastic particles ($\approx 18\%$ vol. fraction). The material parameters were chosen according to Michel and Suquet [11]. For the inclusions they are set to the ones of Boron ($E = 400$ GPa, $\nu = 0.2$). The matrix material is aluminium with nonlinear isotropic hardening of the type

$$\sigma_F(q) = \sigma_0 + hq^m, \quad (15)$$

with q a strain like hardening variable resembling the equivalent plastic strain and the material parameters $\sigma_0 = 75$ MPa, $h = 416.5$ MPa and $m = 0.3895$. The elastic parameters were given by the Young's modulus $E = 75$ GPa and the Poisson's ratio $\nu = 0.3$. The large degree of nonuniformity of the plastic strain field, the displacement field and the

stress field is exemplified in Fig. 5 for the first inelastic mode (scales normalized) which has been identified from a numerical test at macroscopic strain rate

$$\dot{\bar{\boldsymbol{\varepsilon}}} = \frac{\dot{\bar{\varepsilon}}_0}{2} \begin{pmatrix} 2 & 0 & 0 \\ 0 & -1 & 0 \\ 0 & 0 & -1 \end{pmatrix} \mathbf{e}_i \otimes \mathbf{e}_j. \quad (16)$$

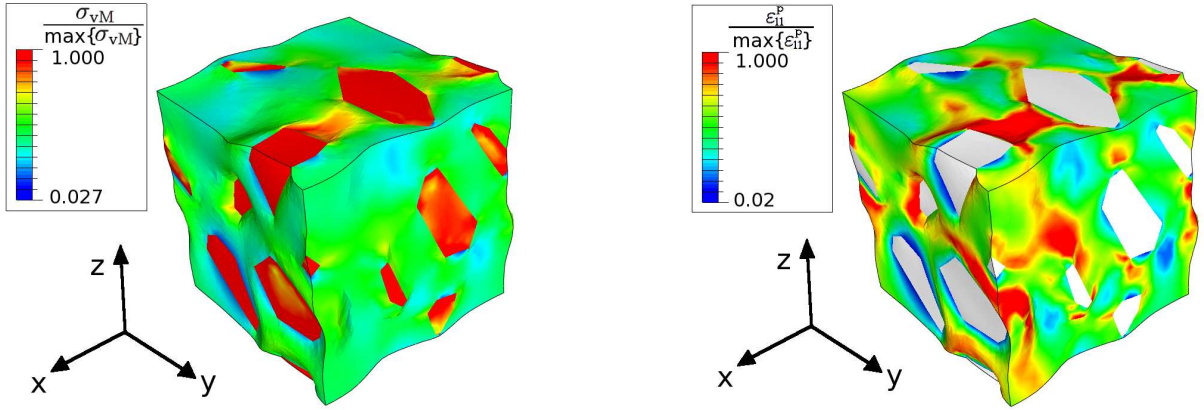


Fig. 5: Plastic Mode 1: von Mises stress σ_{vM} (left) and plastic strain component ε_{11}^P (right)

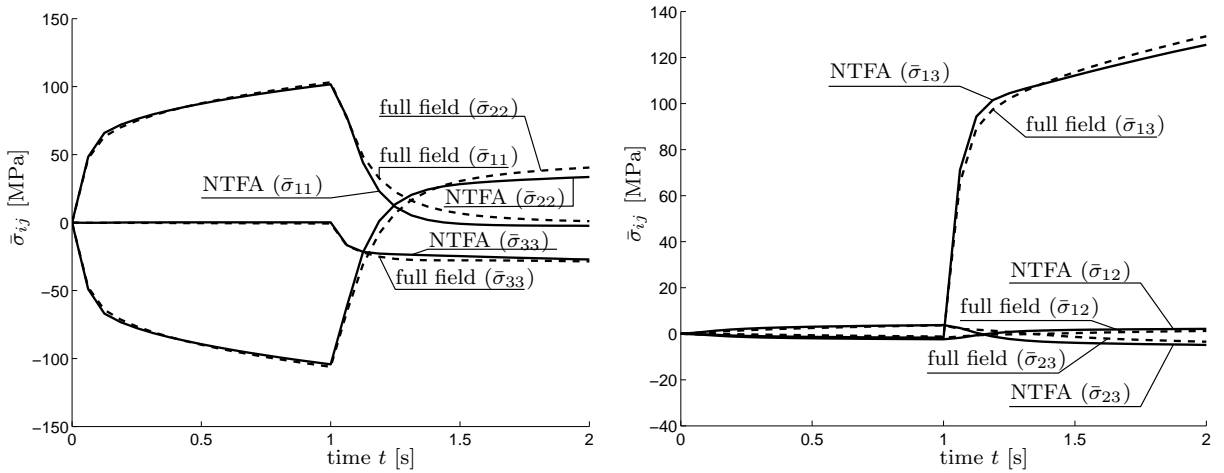


Fig. 6: Time history of $\bar{\sigma}_{11}, \bar{\sigma}_{22}, \bar{\sigma}_{33}$ (left) and $\bar{\sigma}_{12}, \bar{\sigma}_{13}, \bar{\sigma}_{23}$ (right)

The time history of macroscopic stress tensor of the full field computation $\bar{\boldsymbol{\sigma}}^{\text{ref}}$ and the NTFA $\bar{\boldsymbol{\sigma}}^{\text{NTFA}}$ are compared in Fig. 6. The diagonal components (Fig. 6; left) and the shear components (Fig. 6; right) have been separated for clarity.

A considerable agreement was found for the components of the macroscopic stress despite the partial load reversal (particularly in the $\mathbf{e}_2 \otimes \mathbf{e}_2$ -direction; see (14)). While the components of $\bar{\boldsymbol{\sigma}}$ of the NTFA show some discrepancy versus the reference computation it has to be pointed out that the relative errors with respect to $\|\bar{\boldsymbol{\sigma}}\|$ is in the order of 2% and smaller. Hence, the method can be considered to yield acceptable results for partial load reversal and multi-axial loading.

4.2 Structural computation

The homogenized material has been used to model a tension test on the three-dimensional specimen shown in Fig. 7. Since the homogenized material is no longer per se isotropic, it is not possible to reduce the model of the axisymmetric specimen to two dimensions. The discretization of the specimen was (Fig. 7, middle) consists of approximately 70000 nodes, i.e. a total of 220000 degrees of freedom were considered. Kinematic boundary conditions (Fig. 7, right) were prescribed to replicate a standard tension test in e_2 -direction. The total displacement u_y at the end of the load step was set to 1mm equating to 5% of the measured section. The force displacement curve of the microheterogeneous material is shown in Fig. 8.

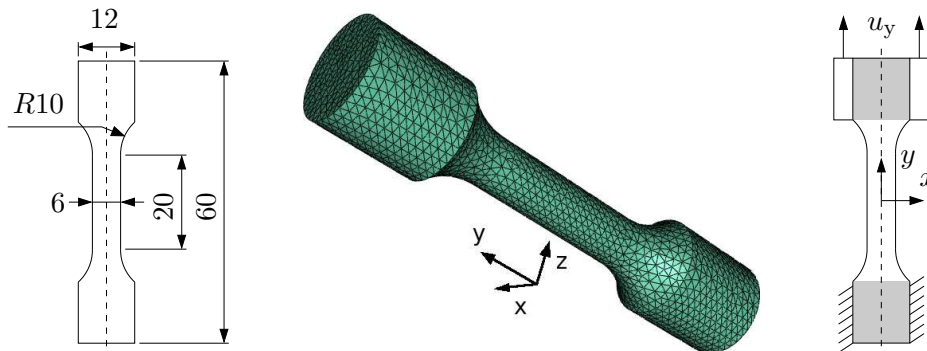


Fig. 7: Threedimensional tensile specimen: Geometry (unit: mm; left), spatial discretization (middle) and boundary conditions (right)

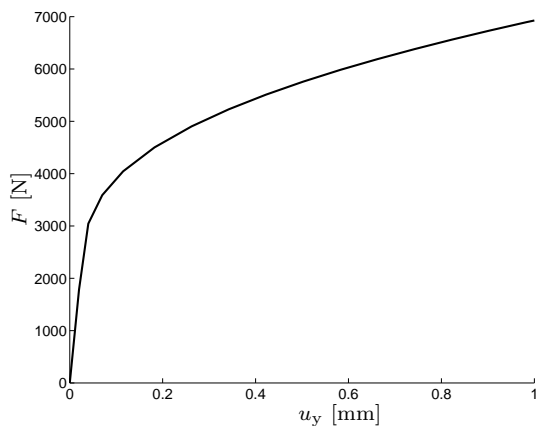


Fig. 8: Force displacement curve

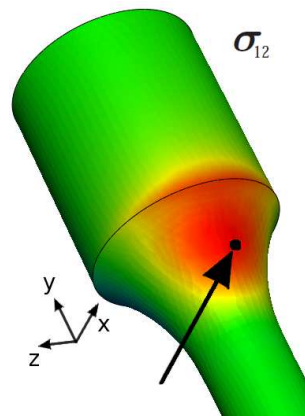


Fig. 9: Observed integration point

The computation was used to validate the implementation of the homogenized material model into the Finite Element code ABAQUS/STANDARD. Particularly, the tangent stiffness operator was tested and the formulation used in the UMAT (User Material Subroutine) allowed for a good convergence rate. During the analysis the stresses, the strains and internal variables computed for the homogenized material model were recorded for the integration point highlighted in Fig. 9. The recorded strain-path was then used to model nonproportional loading on the unit cell level. A full field simulation on the microscale is then carried out to compare the (effective) stress field of the numerical full field simulation to the predicted field from the NTFA. The results are shown in Fig. 10.

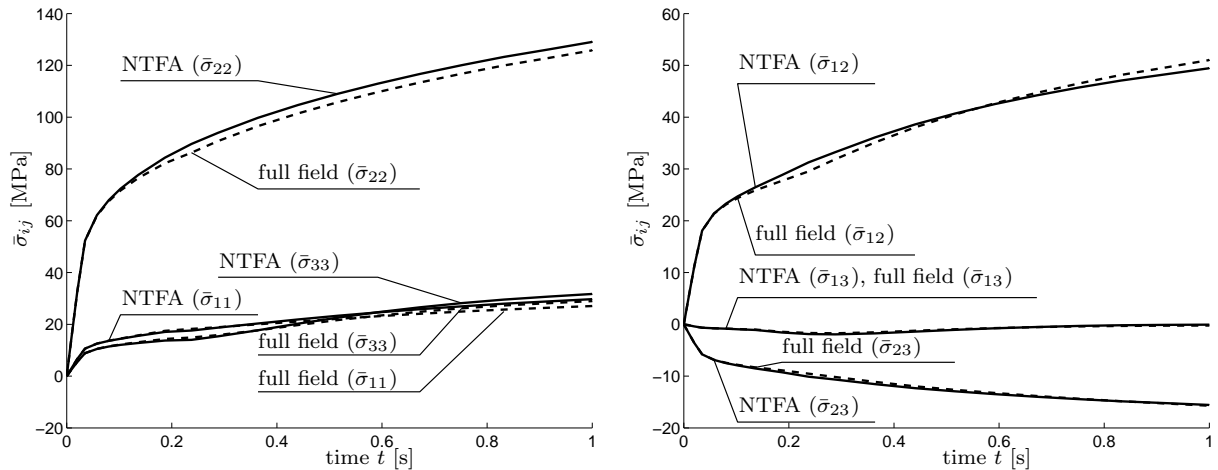


Fig. 10: Time history of $\bar{\sigma}_{11}$, $\bar{\sigma}_{22}$, $\bar{\sigma}_{33}$ (left) and $\bar{\sigma}_{12}$, $\bar{\sigma}_{13}$, $\bar{\sigma}_{23}$ (right)

5 SUMMARY AND CONCLUSIONS

5.1 Summary

An algorithm for the generation of random three-dimensional model microstructures was discussed in Section 2. The procedure has the advantage that particles have a constant distance to each other and arbitrarily high volume fractions are possible. The latter is a critical point for many other algorithms. Moreover, the mesh density is fully adjustable while the geometric representation of the material remains exact which is a disadvantage of the multi-phase element method used by many authors.

The formulation of the NTFA as presented by Michel and Suquet [11] has briefly been revisited in Section 3. The behaviour of the method upon nonproportional loading has numerically been investigated in terms of a comparison between a full field simulation at unit cell level and the results predicted by the NTFA. A number of only five inelastic modes was employed and found to yield a good agreement between the full field simulation and the result predicted by the homogenized material model. Notably the number of degrees of freedom in the NTFA model is six (five mode coefficients, one hardening variable) whereas 200000 displacement degrees of freedom plus a comparably large number of internal variables was solved.

5.2 Conclusions

The NTFA introduced by Michel and Suquet [11] has been extended to (i) three space dimensions with consideration of complexly shaped particles and (ii) implementation using the finite element method. It could be shown that the NTFA shows promising results even in the case of non-proportional three-dimensional loading. The good agreement between reference computations and the NTFA which was found by Michel and Suquet [11, 12], Roussette et al. [13] for two-dimensional problems can be confirmed for three dimensions and more complex microstructures.

In addition to unit cell computations a structural computation using the homogenized material model was conducted. The strain-path has been recorded at an integration point in a region where three-axial loading is to be expected. This strain-path has then been

used to prescribe boundary conditions on the unit cell level. The agreement in the stress field found using the two methods was excellent. It, hence, seems reasonable to use this model for other structural computations where the loading is applied almost proportional.

The implementation used in this work was based on the finite element method which offers the advantage of standardized implementation into commercial software (here: ABAQUS). This approach differs significantly from the Fast Fourier Transform (FFT) used in Michel and Suquet [11, 12], Roussette et al. [13]. We consider the finite element method more suitable for many three-dimensional problems since, given a geometrically exact discretization of the microstructure, there are no volumetric errors and all geometric details, i.e. corners, small edges etc., are considered. The FFT method and block-structured meshes with multi-phase elements have at best the resolution $h = \sqrt[3]{V/N_{\text{DOF}}}$ (V : volume of unit cell, N : number of elements in each coordinate direction). Hence, the number of degrees of freedom quickly increases with these methods if only one characteristic length in the microstructure gets small.

REFERENCES

- [1] S. Nemat-Nasser and M. Hori. *Micromechanics: Overall properties of heterogeneous materials*. Elsevier, 1999.
- [2] J.R. Willis. Bounds and self-consistent estimates for the overall properties of anisotropic composites. *Journal of the Mechanics and Physics of Solids*, 25:185–202, 1977.
- [3] T. Mori and K. Tanaka. Average Stress in a Matrix and Average Elastic Energy of Materials with Misfitting Inclusions. *Acta Metallurgica et Materialia*, 23:571–574, 1973.
- [4] E. Kröner. Berechnung der elastischen Konstanten der Vielkristalls aus den Konstanten des Einkristalls. *Z. Phys.*, 151:504–518, 1958.
- [5] F. Fritzen, T. Böhlke, and E. Schnack. Periodic three-dimensional mesh generation for crystalline aggregates based on voronoi tessellations. *Computational Mechanics*, 43(5):701, 2009. doi: 10.1007/s00466-008-0339-2.
- [6] C. Miehe. Strain-driven homogenization of inelastic microstructures and composites based on an incremental variational formulation. *Journal for Numerical Methods in Engineering*, 55:1285–1322, 2002.
- [7] F. Feyel. A multilevel finite element method (FE²) to describe the response of highly non-linear structures using generalized continua. *Computer Methods in Applied Mechanics and Engineering*, (192):3233–3244, 2003.
- [8] G.J. Dvorak and Y. Benveniste. On transformation strains and uniform fields in multiphase elastic media. *Proceedings of the Royal Society of London A*, (437):291–310, 1992.
- [9] G.J. Dvorak, Y.A. Bahei-El-Din, and A.M. Wafa. The modeling of inelastic composite materials with the transformation field analysis. *Modelling and Simulation in Material Science and Engineering*, (2):571–586, 1994.

- [10] P. Suquet. *Continuum micromechanics*, volume 377 of *CISM Lecture Notes*, pages 197–264. Springer Verlag (New York), 1997.
- [11] J.C. Michel and P. Suquet. Nonuniform transformation field analysis. *International Journal of Solids and Structures*, (40):6937–6955, 2003.
- [12] J.C. Michel and P. Suquet. Computational analysis of nonlinear composite structures using the nonuniform transformation field analysis. *Computer Methods in Applied Mechanics and Engineering*, (193):5477–5502, 2004.
- [13] S. Roussette, J.C. Michel, and P. Suquet. Nonuniform transformation field analysis of elastic-viscoplastic composites. *Composite Science and Technology*, 69:22–27, 2009. doi: 10.1016/j.compscitech.2007.10.032.
- [14] F. Barbe, L. Decker, D. Jeulin, and G. Cailletaud. Intergranular and intragranular behavior of polycrystalline aggregates. Part 1: F.E. Model. *International Journal of Plasticity*, 17:513–536, 2001.
- [15] A. Miserez, A. Rossoll, and A. Mortensen. Investigation of crack-tip plasticity in high volume fraction particulate metal matrix composites. *Engineering Fracture Mechanics*, (71):2385–2406, 2004.
- [16] F. Aurenhammer. Voronoi Diagrams - A survey of a Fundamental Geometric Data Structure. *ACM Computing Surveys*, 23(3):345–405, 1991.
- [17] J. Ohser and F. Mücklich. *Statistical Analysis of Microstructures in Materials Science*. Statistics in Practice. John Wiley & Sons, 2000.
- [18] F. Fritzen and T. Böhlke. Homogenization of the physically nonlinear properties of three-dimensional metal matrix composites using the nonuniform transformation field analysis. Proceedings of the 17th International Conference on Composite Materials, 2009.